

Hardware Development of a MIMO Pseudo E-SDM System and Real-time Channel Emulator

Julian Webber, Toshihiko Nishimura, Takeo Ohgane and Yasutaka Ogawa
 Hokkaido University, Sapporo 060-0814 Hokkaido Japan
 E-mail: julian.webber@m-icl.ist.hokudai.ac.jp

Abstract—When channel state information is fed-back to the transmitter, multiple-input multiple-output (MIMO) systems can realize eigenbeam-space division multiplexing (E-SDM) and system performance can be improved. Pseudo E-SDM offers both reduced computational complexity (the mean number of multiplications for 4×4 is reduced to about 1/10) and a reduction in the effective channel delay spread compared to E-SDM. This work describes the design of such a MIMO orthogonal frequency division multiplexing (OFDM) system based on the IEEE802.11n standard. The paper describes the real-time processing on field programmable gate arrays (FPGA) capable of sustaining a maximum 260 Mbps service within a 20 MHz bandwidth and the MIMO signal processing computed on digital signal processors (DSP). The modified Jakes model permits the Rayleigh fading channel to be emulated in real-time with limited hardware complexity.

I. INTRODUCTION

The continually increasing requirements for higher data-rate communications together with the finite bandwidth resource have generated extensive research into methods to maximize the achievable capacity of practical wireless systems. Multiple input multiple output (MIMO) systems have been the focus of much research in the last decade e.g. [1]. MIMO-OFDM systems exploit both the diversity gains provided from multiple antennas as well as the benefits of orthogonal frequency domain multiplexing (OFDM) systems that operate in a wide-band channel without inter-symbol interference.

The IEEE 802.11n specification is the international standard for MIMO-OFDM systems. The draft standard specifies 76 different modulation coding schemes (MCS) each for the 20 MHz and 40 MHz modes [2] using upto 4 substreams. Fig. 1 charts the data-rate and number of antennas versus MCS assuming a $0.8 \mu\text{s}$ guard interval. The maximum burst bit rate is 260 Mbps, and is achieved using four 64-QAM substreams. The communications system described here is based on a 20 MHz transmission bandwidth and 800 ns guard interval. There are 52 data, 4 pilot, 1 DC and 7 null subcarriers per 64-point FFT.

II. E-SDM

Eigenbeam-Space Division Multiplexing (E-SDM) is the optimum method to transmit data through orthogonal channels based on subspace decomposition of the known channel. At the transmitter, an input stream is divided into K substreams ($K \leq \min(N_{\text{tx}}, N_{\text{rx}})$), where N_{tx} and N_{rx} are the number of transmit and receive antennas respectively. Signals before transmission are shaped by a transmit weight matrix \mathbf{W}_{tx} to

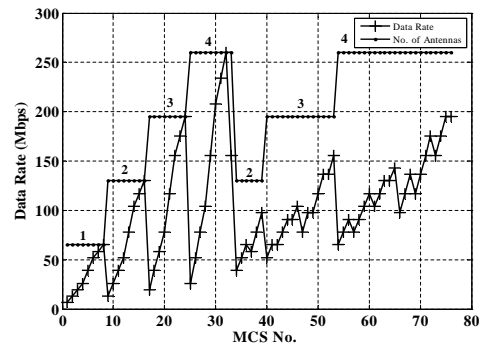


Fig. 1. Data rate and number of substreams vs. MCS for IEEE802.11n systems (20 MHz bandwidth and $0.8 \mu\text{s}$ guard interval).

form orthogonal beams and control power allocation. At the receiver, signals are detected by a receive weight matrix \mathbf{W}_{rx} . The optimal \mathbf{W}_{tx} and \mathbf{W}_{rx} are determined by [3] as:

$$\mathbf{W}_{\text{tx}} = \mathbf{U}\sqrt{\mathbf{P}}, \quad (1)$$

$$\mathbf{W}_{\text{rx}} = \mathbf{U}^H \mathbf{H}^H, \quad (2)$$

where $\mathbf{U} \in \mathbb{C}^{N_{\text{rx}} \times K}$ is obtained by eigen decomposition as:

$$\mathbf{H}^H \mathbf{H} = \mathbf{U} \mathbf{\Lambda} \mathbf{U}^H, \quad (3)$$

$$\mathbf{\Lambda} = \text{diag}(\lambda_1, \dots, \lambda_K). \quad (4)$$

Here, $\lambda_1 \geq \lambda_2 \geq \dots \geq \lambda_K > 0$ are the eigenvalues of $\mathbf{H}^H \mathbf{H}$. The columns of \mathbf{U} are the eigenvectors corresponding to the eigenvalues, and $\mathbf{P} = \text{diag}(P_1, \dots, P_K)$ is the transmit power matrix.

The detected signals in an ideal E-SDM system, in which the transmit weight matrix completely matches an instantaneous MIMO channel response, are given by

$$\mathbf{y}(t) = \mathbf{\Lambda}\sqrt{\mathbf{P}}\mathbf{s}(t) + \mathbf{W}_{\text{rx}}\mathbf{n}(t), \quad (5)$$

where $\mathbf{s}(t) \in \mathbb{C}^K$ is a signal vector consisting of signals $s_1(t), \dots, s_K(t)$ sent through the K subchannels, and $\mathbf{n}(t) \in \mathbb{C}^{N_{\text{rx}}}$ is noise at the RX. The result from (5) shows that the E-SDM technique transforms the MIMO channel into K orthogonal subchannels. However, conventional singular value decomposition (SVD) includes a phase ambiguity, and as the transmit weights are individually computed at each sub-carrier they exhibit a random phase rotation, which enlarges the effective channel delay spread.



Fig. 2. Transmitter, channel emulator and receiver systems each consisting of a Koden E-1071 signal processing platform.

To calculate the pseudo-eigenvector achieving frequency correlation we first compute the auto-correlation of the estimated channel as (6) [4]:

$$\mathbf{R}_{\text{rx}}(t) = \frac{1}{\sqrt{Q}} \sum_{t=0}^{T_d} \mathbf{H}_T(t) \mathbf{H}_T^H(t + \tau) \quad (6)$$

where τ is the delay lag, Q is the FFT size and $\mathbf{H}_T(t)$ is the time domain channel impulse response. The sum of the diagonal elements of $\mathbf{H}_T \mathbf{H}_T^H$, $\text{tr}[\mathbf{R}_{\text{rx}}(0)]$, represents the total energy of the channel, and $\mathbf{R}_{\text{rx}}(0)$ is equal to the sum of $\mathbf{H}_F(f) \mathbf{H}_F^H(f)$ over all frequencies, where \mathbf{H}_F is the frequency domain channel. The eigen-vector decomposition (EVD) of $\mathbf{R}_{\text{rx}}(0)$ is given by (7):

$$\mathbf{R}_{\text{rx}}(0) = \mathbf{V}_{\text{rx}} \mathbf{\Lambda}_{\text{rx}} \mathbf{V}_{\text{rx}}^H, \quad (7)$$

where $\mathbf{\Lambda}$ contains descending ordered eigenvalues of $\mathbf{R}_{\text{rx}}(0)$, and \mathbf{V}_{rx} is a unitary matrix. The receive weight matrix is given by \mathbf{V}_{rx}^H and the TX matrix is obtained from the Gram-Schmidt (GS) orthonormalization as in (8) [4]:

$$\mathbf{W}_{\text{tx}} = GS[\mathbf{H}_F^H(f) \mathbf{V}_{\text{rx},K}] \quad (8)$$

The mean number of complex multiplications for 4×4 PE-SDM compared to E-SDM is reduced to approximately 1/10 and is slightly reduced for the 2×2 case [4], though the computation times depend on the particular channel fading.

III. SYSTEM CONFIGURATION

A Koden E-1071 signal processing system [5] is deployed for each of the transmitter, channel emulator and receiver (Fig. 2). The Koden E-1071 contains a back-plane to which a number of signal processing boards are interconnected. Each system comprises an identical PC, clock generation and DSP cards. The DSP card contains the Xilinx Virtex-4 LX100, SX55 and FX60 FPGAs linked to four inter-connected Analog Devices TigerSharc TS-201 DSPs. The transmitter system additionally contains a signal conditioning card with eight 130 MHz DACs, four SX55 FPGA and one LX100 FPGA. The receiver system includes a similar signal-conditioning card but with eight 135 MHz ADCs. The channel emulator system contains both ADC and DAC cards.

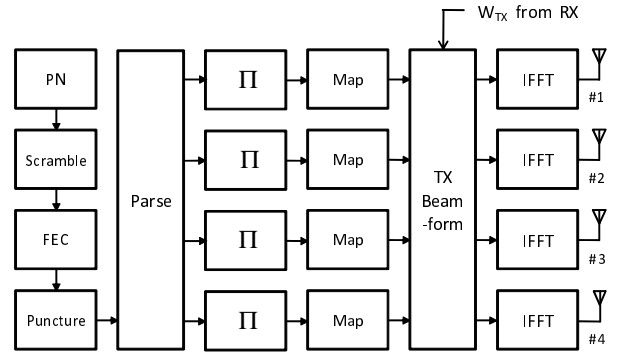


Fig. 3. Transmitter block diagram.

IV. TRANSMITTER SYSTEM

The transmitter system block diagram is shown in Fig. 3. The code for each block is written in a hardware description language (HDL). The user data generated is scrambled using a feedback shift register and 1/2-rate convolutionally encoded using forward error correction (FEC). The parser distributes groups of bits onto different substreams and the interleaver maps bits across non-adjacent subcarriers. After puncturing, the mapper takes 2, 4 or 6-bits consecutive bits and creates a QPSK, 16-QAM or 64-QAM symbol respectively.

The transmitter beamformer weights are derived from the channel state information (CSI) estimates computed in the receiver. The weights are transferred to the TX FPGA and multiplied with the mapper output. The 64-point radix-4 IFFT converts the frequency domain data from the beamformer output into a time domain signal. A $0.8 \mu\text{s}$ guard interval is inserted and as its duration is greater than the longest multipath delay, inter-symbol interference (ISI) is prevented. The blocks are pipelined to reduce the maximum clock speed within each module. For example, the IFFT and interleaver for symbol N , is computed at the same time as the convolutional encoder is processing symbol $N - 1$.

V. RECEIVER SYSTEM

The main components of the receiver are shown in Fig. 4. The coarse timing module locates the approximate frame start by computing the auto-correlation of the received sequence with a delayed version. A 160-sample plateau is formed due to the ten consecutive preamble short training fields each of length sixteen samples (Fig. 5). During fine-timing recovery the received signal is cross-correlated with the preamble over a localized search window containing the long training field.

The received time-domain signal is processed by a radix-2 64-point FFT to generate the frequency domain signal. The CSI is estimated in the frequency domain by comparing the received preamble with the known transmitted version. The CSI estimates are accessed by either the Rx DSP in order to compute the channel eigen-analysis or a second Rx FPGA co-processor that computes the zero-forcing (ZF) complex channel inversion by QR decomposition.

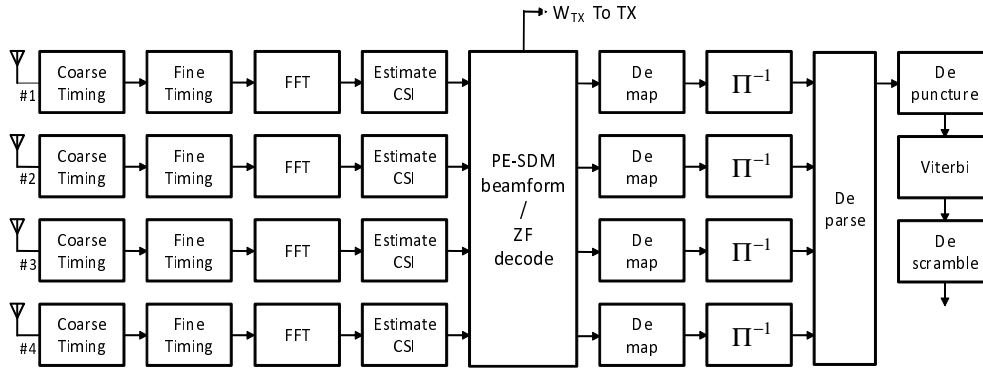


Fig. 4. Receiver block diagram.

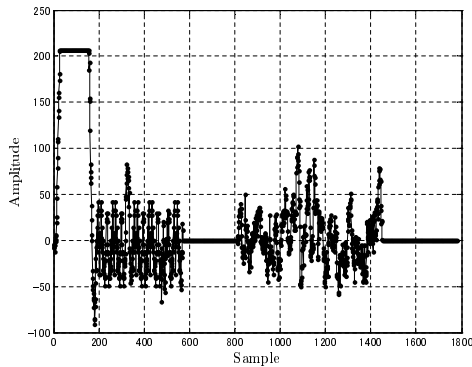
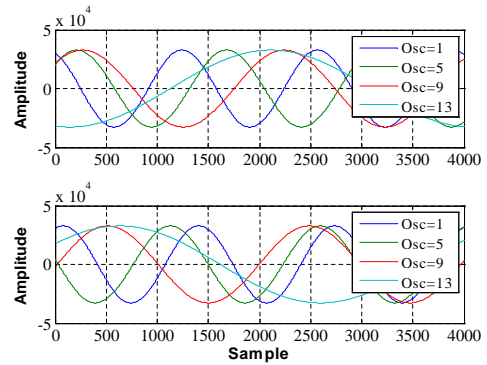


Fig. 5. Coarse timing correlator output signal.


 Fig. 6. (top) $\cos(\beta_n + \theta_n + \omega_n t)$, (bottom) $\cos(\beta_n - \theta_n - \omega_n t)$

The deparser demultiplexes the substream data into a single data-train in a round-robin process. The deparsed signal and corresponding depuncturing sequence are inputs to the Viterbi module. The decoder takes as input a soft four-bit signal and computes over a trace-back length of 84 samples.

VI. CHANNEL EMULATOR DESIGN

The Jakes model assumes that N equal-strength rays arrive at a moving receiver with uniformly distributed angles of arrival, α_n , such that ray n experiences a Doppler shift $\omega_n = \omega_M \cos(\alpha_n)$, where $\omega_M = 2\pi f v / c$, v is the vehicle speed, c is the speed of light and f is the carrier frequency. The initial random phase of each ray is distributed between 0 and 2π [7]. In the modified Jakes model of [8], orthogonal Hadamard codes determine whether the rays add constructively or destructively, and is described by (9):

$$T(t, k) = \sqrt{\frac{2}{N}} \sum_{n=1}^N H_{kn} \{ [\cos(\beta_n) + j \sin(\beta_n)] \cos(\omega_n t + \theta_n) \} \quad (9)$$

where H_{kn} is the Hadamard code sequence and N is the number of oscillators.

The offset phase β_n is distributed over $[0, \pi)$. The outputs of four cosine generators computing $\cos(\beta_n + \theta_n + \omega_n t)$ and $\cos(\beta_n - \theta_n - \omega_n t)$ are shown in Fig. 6 top and bottom respectively for oscillators $n=1,5,9,13$. The characteristic fading

envelopes for $H_{11}, H_{21}, H_{31}, H_{41}$ can be seen after the Hadamard weighting of the N signals (Fig. 7).

The ADC input signals $x_0(t)$ to $x_3(t)$, are sampled and convolved with the four channels $h_{00}(t), h_{10}(t), h_{20}(t)$ and $h_{30}(t)$ respectively. The four resultant signals are summed and a single AWGN sample added to form the output signal $y_0(t)$. This process is repeated to create the remaining three output signals $y_1(t)$ to $y_3(t)$.

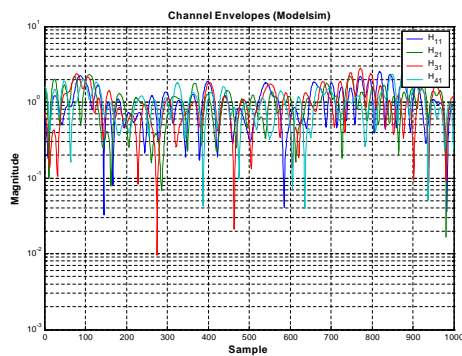
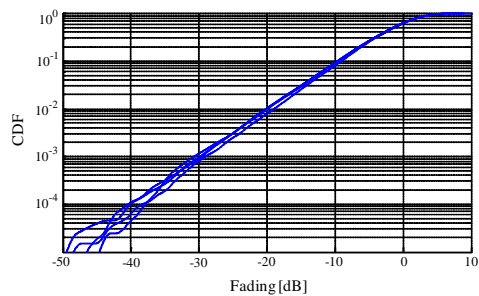
A uniform random number, $X_n(0), \dots, X_n(J-1)$ is generated from the outputs of J different M-sequence generators at the n -th symbol timing. Additive white Gaussian noise Y_n is created by summing the outputs of L uniform noise generators [9] (10):

$$Y_n = \frac{\sqrt{L}}{\sigma} \frac{1}{L} \sum_{k=0}^{L-1} X_{n,k} - \mu \quad (10)$$

where μ and σ^2 are the mean value and the variance of X_n , respectively. The variables J and L can be varied to balance the accuracy and complexity. Fig. 8 shows the CDF statistics for a 2×2 MIMO Rayleigh fading channel. The results are accurate at the high power region from above about -30 dB.

VII. SYSTEM PERFORMANCE

The error performances of the SDM algorithms were simulated for a system based on the IEEE802.11n standard. Eight


 Fig. 7. Channel envelopes H_{11} , H_{21} , H_{31} , H_{41} (Modelsim data).

 Fig. 8. CDF of 2×2 MIMO Rayleigh fading channels using PN generator.

coded bits were assigned per OFDM symbol on each subcarrier. The per substream allocated bit patterns were therefore $[2,2,2,2]$, $[6,2,0,0]$, $[4,2,2,0]$ or $[4,4,0,0]$ and correspond to MCS values 25, 34, 39 and 11 respectively. The FEC coding rate was $1/2$, and hence all four MCS modes here provide a 52 Mbps aggregate service.

The channel consisted of three sample spaced paths with average 8 dB decaying. The receiver estimated the channel based on the known preamble and calculated the optimum weights. The ZF and SVD weights were determined based on MIMO channel estimates from the previous packet.

Fig. 9 show the BER performance versus normalized total TX power for three E-SDM systems. The normalized TX power is the total TX power normalized to the TX power yielding an average E_s/N_0 of 0 dB in the single antenna case in the same fading channel. SDM with equal power on each substream provides the least performance for both 2×2 and 4×4 systems. E-SDM gives the optimum performance very closely followed by PE-SDM.

The 4×4 PE-SDM weight computation time was profiled on the 500 MHz TS201 DSP with results shown in (TABLE I). The total number of clock cycles per frame corresponded to 3.18 ms of processing time, which is within the channel coherence time.

VIII. CONCLUSION

This paper has described the design of a MIMO-SDM and channel emulator system based on the draft IEEE802.11n standard. Initial results have shown the efficacy of the PE-

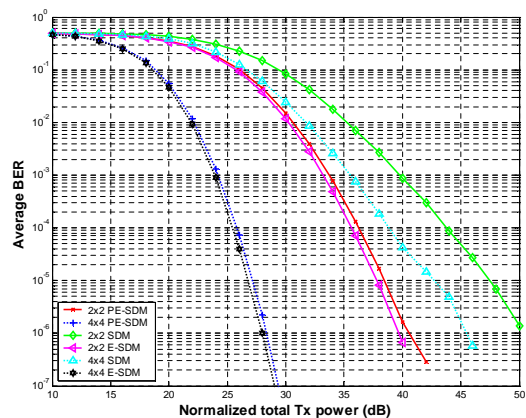


Fig. 9. SDM system performances in channel-B

 TABLE I
PE-SDM COMPLEXITY ON TS201 DSP (4×4).

Function	Cycles / s.c.	Av. Cycles/DSP (13 s.c./DSP)
RxCrf0()	200,601	50,150
Hemitian	507	6,591
Xcorr ($\times 2$)	73,156	951,028
Gram-Schmidt	36,944	480,272
Other	7,843	101,959
Total	319,051	1,590,001

SDM algorithm and future work will study the PE-SDM performance in a large variety of channel conditions and in much reduced time compared to software simulations.

ACKNOWLEDGMENT

This work was supported by the Strategic Information and Communications R&D Promotion Programme from the Ministry of Internal Affairs and Communications, Japan and the Global Centre of Excellence program. The authors would also like to thank Koden Electronics.

REFERENCES

- [1] G. J. Foschini and M. J. Gans, "On limits of wireless communications in a fading environment when using multiple antennas," *Wireless Pers. Commun., Springer*, vol. 6, pp. 311–335, Mar. 1998.
- [2] "IEEE P802.11 Wireless LANs Joint Proposal: High throughput extension to the 802.11 Standard: PHY," IEEE 802.11-05/1102r4, Jan. 2006.
- [3] T. Ohgane, T. Nishimura, and Y. Ogawa, "Applications of space division multiplexing and those performance in a MIMO channel," *IEICE Trans. Commun.*, vol. E88-B, no. 5, pp. 1843–1851, May 2005.
- [4] H. Nishimoto, T. Nishimura, T. Ohgane, and Y. Ogawa, "Pseudo eigenbeam-space division multiplexing (PE-SDM) in frequency-selective MIMO channels," *IEICE*, vol. E90-B, pp. 3197–3207, Nov. 2007.
- [5] Koden. "E-1072 signal processing platform," Koden Electronics, 2008.
- [6] T. Chiueh and P. Tsai. "OFDM baseband receiver design for wireless communications," Wiley Press, 2007.
- [7] W. C. Jakes, *Microwave Mobile Communications*, Wiley, 1974.
- [8] P. Dent, G. Bottomley and T. Croft, "Jakes fading model revisited," *Electronics Letters*, vol. 29, no. 13, pp. 1162–1163, June 1993.
- [9] M. Cui, H. Murata and K. Araki, "Real-time MIMO Received Signal Generator for Spatial Multiplexing Systems," *Proc. IEEE VTC 2004*, pp. 4345–4348, Nov. 2004.